CIRP Journal of Manufacturing Science and Technology 30 (2020) 1–11

Contents lists available at ScienceDirect

CIRP Journal of Manufacturing Science and Technology

journal homepage: www.elsevier.com/locate/cirpj

Real time monitoring and control of friction stir welding process using multiple sensors

Debasish Mishra[a], Abhinav Gupta[b], Pranav Raj[b], Aman Kumar[b], Saad Anwer[b], Surjya K. Pal[c,*], Debashish Chakravarty[d], Srikanta Pal[b], Tapas Chakravarty[e], Arpan Pal[e], Prateep Misra[e], Sudip Misra[f]

[a] Advanced Technology Development Centre, Indian Institute of Technology Kharagpur, India
[b] Department of Electronics and Communication Engineering, Birla Institute of Technology Mesra, India
[c] Department of Mechanical Engineering, Indian Institute of Technology Kharagpur, India
[d] Department of Mining Engineering, Indian Institute of Technology Kharagpur, India
[e] TATA Consultancy Services Research and Innovation, Kolkata, India
[f] Department of Computer Science & Engineering, Indian Institute of Technology Kharagpur, India

ARTICLE INFO

Article history:
Available online 17 April 2020

Keywords:
Friction stir welding
Industry 4.0 in manufacturing
Real time control
Multiple sensors
Cloud computing
Signal processing
Machine learning

ABSTRACT

In the present work, a novel cloud-based remote and real time monitoring and control scheme has been developed for a manufacturing process named friction stir welding (FSW) to avoid occurrence of weld defects. This model acquires data from multiple sensors associated with the FSW machine and transmits them to the cloud. The signals are analyzed and processed in the cloud in real time through various signal processing and machine learning techniques. The model provides a feedback to the machine regarding the desired controlled parameters to achieve an improved weld quality. This is an example of Industry 4.0 where a manufacturing process can be controlled in real time from any location.

Introduction

The importance of real time process monitoring lies in observing few characteristics of a process identified by the domain expert. In order to appreciate the outcome of real time monitoring of any process, it must be accompanied by a control scheme. It is worth noting that significant investment on infrastructure is required to cater manufacturing and embedding of sensors for monitoring the process. In addition, the product quality has to be ensured with a closed-loop control scheme available for that process. The sensor-based monitoring and subsequent control can reduce manual contribution, make the manufacturing process more maintainable, flexible, error-free and cost-effective. It also results in enhanced efficiency and product quality. This article mentions about one such novel monitoring and control scheme developed for an advanced welding technique named, friction stir welding (FSW). The article attempts at addressing two features, (a) developing a closed-loop system for FSW, and (b) making FSW process compliant with *Industry 4.0*. Both these features have been developed and implemented simultaneously. The *Industry 4.0*, i.e. the fourth industrial revolution, revolves around the concepts of Internet of Things, data analytics, cloud computing etc. In short, *Industry 4.0* aims at digitization for extraction of meaningful information from the sensory data. While *Industry 4.0* can be considered as a big umbrella of several concepts, automation is one major concept. The following paragraph gives a highlight of the previous works on FSW.

For monitoring of FSW process, several physical parameters such as force, torque, acoustic emission (AE), and current signatures have been utilized. The welding defects were identified by analyzing axial force and torque signals in time-frequency domain [1,2]. Mean of square of errors and variance were the features extracted from the signals. *"Gap defects"* referred as voids in joint line were identified by analyzing axial force and AE signals [3,4]. While inferences were drawn from force signal in time domain, AE signal was studied in time-frequency domain. Other than axial force, thrust and feed forces were utilized for classification of weld quality, where the frequency spectrum of force signal of the defective weld was found to have higher

* Corresponding author at: Department of Mechanical Engineering, Indian Institute of Technology Kharagpur, Kharagpur 721302, India.
E-mail address: skpal@mech.iitkgp.ac.in (S.K. Pal).

https://doi.org/10.1016/j.cirpj.2020.03.004
1755-5817/

amplitude in the lowest frequency bin as compared to the spectrum of defect-free weld [5]. AE signal was also acquired for analyzing the effect of varying tool pin profiles [6]. Features such as energy and amplitude were extracted from the signal. In another work, the ultimate tensile strength (UTS) of the joint was predicted using voltage and current signatures of spindle and feed motors and tool rotational speed signature [7]. The current signature of spindle motor was found to have the highest correlation with the UTS. It is worth appreciating these works as they represent state-of-the-art techniques for distinguishing defective and defect-free welds, predicting weld quality etc. However, as the strategies are carried out in an offline manner, they cannot control the process in real time i.e. they cannot avoid the occurrence of defects or improper welding with improper set of parameters, or in case of any sudden damage to the machine.

To bridge this lacuna, several strategies to control FSW process were studied which includes controlling force, torque, and position via tool rotational speed (ω), welding speed (v), and, plunge depth (p). The axial force is significantly affected by small variations in p. This led to usage of p as the variable to control axial force. A proportional integral derivative (PID) controller was used where the servo force controlled loop resided outside the position control loop [8]. The actual force signal was acquired and the error signal was given as feedback to the position controller. Similarly, a PID controller was utilized for torque where its control loop resided outside a position control loop [9]. A rotating type dynamometer was utilized to acquire actual torque and generate the error signal. Although, the variation in p for both torque and axial force control cases was found to be the same, torque has been suggested to be a more sensitive parameter to the changes in p than axial force. A comparative study reports v to be the suitable parameter for controlling axial force amongst ω, v, and p because of the unidirectional dynamics of feed motor which remained unaffected from the load which was being controlled [10]. A comprehensive review of these works can be found in Ref. [11]. The following paragraph outlines the summary of these previous works, and thereby, presents novelty of the present work.

The previous studies involve offline monitoring techniques, and therefore, do not improve the weld quality in real time. In addition, FSW is governed by ω and v, because, change in these values affects frictional heat generation [12]. To develop a reliable architecture, both parameters must be considered, which is lacking in the literature. Moreover, the available control schemes rely on a single sensor which upon malfunctioning can make the process unstable. In this present work, a novel real time monitoring and control scheme is developed for FSW. This scheme acquires data from multiple sensors remotely in a cloud server, processes them via various digital signal processing (DSP) and machine learning (ML) techniques to infer the weld quality and provide feedback to FSW machine. This work is in-line with the goals of *Industry 4.0*, and aims at the creation of a smart FSW factory. As the process is controlled in real time, the occurrence of welding defects can be avoided, and material rejection can be drastically reduced. The entire system has been automated which reduces the usage of human labour. The following section discusses the details about the experiment being performed in the present study.

FSW experimental details

In order to incorporate analytics in the scheme, it was necessary to build a "*knowledge base*" for FSW comprising of several parametric combinations, corresponding sensory data and weld quality. In this study, an aluminium alloy, AA6061 has been chosen as the base material. For the sheets having a thickness of 3 mm with 100 mm × 80 mm dimension, a tool comprising of the following features was used to fabricate the welds: (a) flat shoulder with 18 mm diameter, (b) a conical pin with upper and lower diameters of 6 mm and 4 mm, respectively, and its length being 2.7 mm. The employed tool was fabricated from H13 steel material. The sheets were welded in a butt joint configuration on an instrumented, numerically controlled FSW machine (WS004, ETA Technology) depicted in Fig. 1. The machine has a maximum rated ω of 3000 rpm and v of 1000 mm/min. The control panel attached with machine has a graphical user interface (GUI) where the process parameters for joining such as ω, v, p, start and end positions of the weld are provided as inputs. The depth to which the tool will penetrate is identified prior to the experiment by manually moving the spindle mounted with tool downwards. The tilting (α) of the spindle head is also performed manually. Thus, p and α cannot be controlled online during welding with the present machine configuration. During welding, force, torque, and power signals were acquired as they are typical in the literature of monitoring and control of FSW. Force and torque were acquired from a load cell inbuilt in FSW machine, and power sensor (Montronix, PS100) was connected externally and integrated with the developed interface.

Various defective and defect-free welds were first fabricated, and the acquired information from the three aforementioned sensors was processed offline to predict the weld quality. The prediction idea here was to know from the signal's information, if a

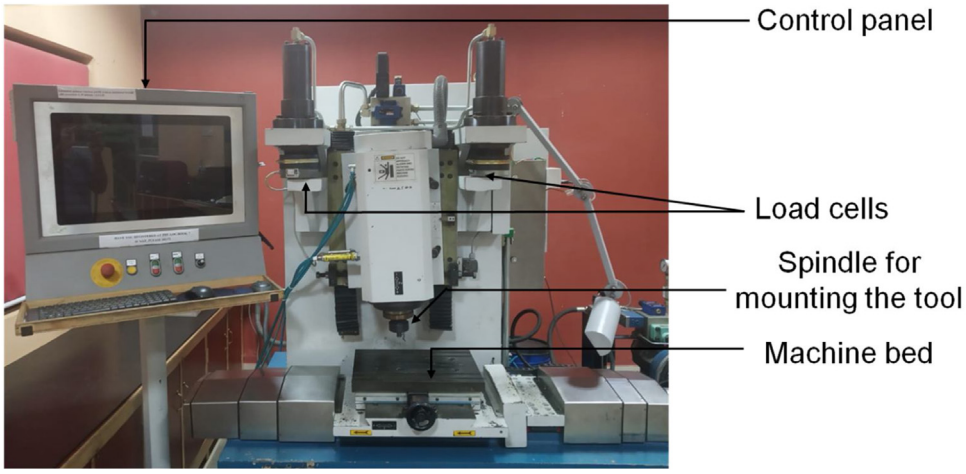

Fig. 1. FSW machine.

Table 1
Process parameters.

ω (rpm)	600, 800, 1000, 1400, 1800, 2200, and 2600
v (mm/min)	40, 50, 60, 80, 100, 150, and 200

weld is free from defect or has defects. The UTS of the samples was also determined, the details of which has been reported in a later sub-section. This study helped in identifying the range of ω and v for achieving defect-free welds. Thereafter, a real-time environment was developed where the information from the three sensors was acquired online, which was used to predict the weld quality, and if found defective, modified parameters were sent to the machine to achieve a weld free from defect. The prediction of weld quality here includes, knowing if a weld is with or without defects, and the UTS of the weld. The modified parameters include new ω and v.

Process parameters

Several trial experiments were performed to identify the range of parameters to be selected for creating the *knowledge base*. As stated previously, p and α cannot be controlled online during welding with the present machine configuration; thus, these two parameters were first fixed. For welding AA6061 sheets in butt joint configuration, α of 2° has been suggested for achieving defect-free welds [13]. These result has been stated both experimentally and numerically. As such, in the present case, a 2° tilt, and p of 0.2 mm were selected. Other parametric combinations included 6 different values of ω and 7 different values of v; constituting a total of 42 welds following a full factorial approach as tabulated in Table 1. The selection of these parameters was based on several trial experiments.

Post-weld study

After fabrication, UTS was determined. Tensile specimen in the direction perpendicular to the welding was cut from the welded samples by using a CNC wire-cut electro discharge machine (Elecktra, Maxicut 523). The standard followed for the specimen is ASTM E8 (sub-size specimen) which has an overall length of 100 mm. A universal tensile testing machine (Instron, 8862) having a capacity of 100 kN was utilized for the test. The crosshead speed during the test was 1 mm/min. Fig. 2 represents the UTS values obtained with the opted parametric combinations. With the range of parameters selected in the present study, maximum UTS of 249.4 MPa is achieved at ω = 1000 rpm and v = 200 mm/min, and the least obtained is 149.2 MPa at ω = 600 rpm and v = 200 mm/min. The UTS of the base AA6061 was 270 MPa. There is no particular trend in the obtained UTS values with respect to increasing values of ω and v. However, few observations can be noted at the lower and higher ends of the range of ω values. At lower value of ω (600 rpm), with increasing values of v from 40 to 100 mm/min, there is an increase in the UTS, however, with further increase to 150 and 200 mm/min, the UTS decreases drastically. This is because of deficiency of frictional heat with such high values of v, which resulted in defective welds. On the other hand, at 2600 rpm, with increasing v, the UTS can be seen to be increasing. The frictional heat increases with increase in ω, and the weld fabricated with ω = 2600 rpm and v = 40 mm/min, had experienced maximum amount of heat content. This heat gradually decreases with increasing values of v, and the optimum UTS has been obtained at a v = 200 mm/min. The motive behind finding the UTS values of the welds was to identify the range of parameters that will yield the maximum and the minimum UTS with respect to base material. The corresponding information acquired from the three sensors with respect to each parametric combination was utilized to build a predictive model for the UTS. Few experiments were repeated for ensuring the results.

Multi-sensor approach

Fig. 3 schematically shows the proposed scheme. A GUI has been created in LABVIEW software which receives data from three sensors and thereby transmits them to cloud by using transmission control protocol/internet protocol (TCP/IP). TCP/IP utilizes a *"client/server"* model where the *"client"* refers to a machine which is provided with service by another computer referred as *"server"*.

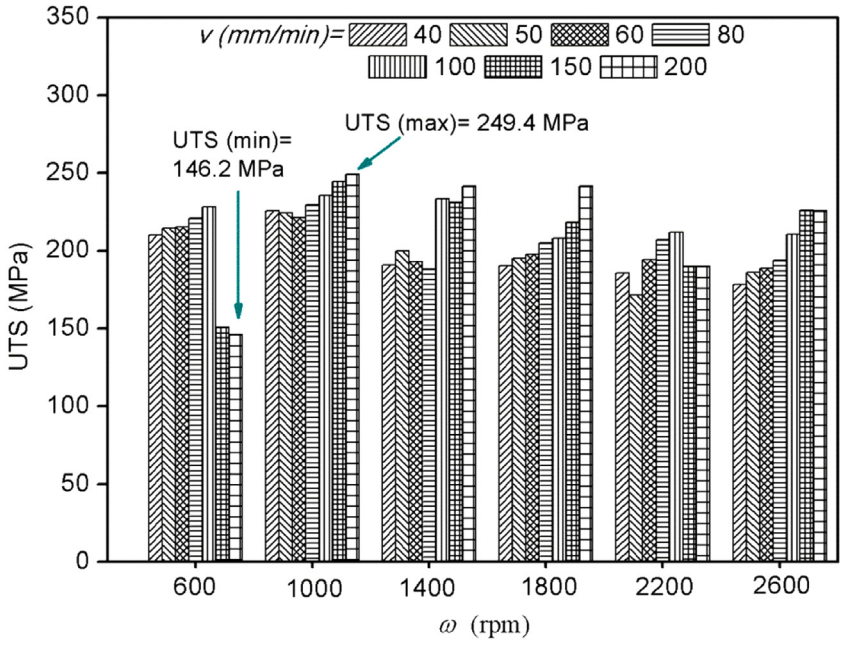

Fig. 2. UTS values of the welds fabricated with opted parametric combinations.

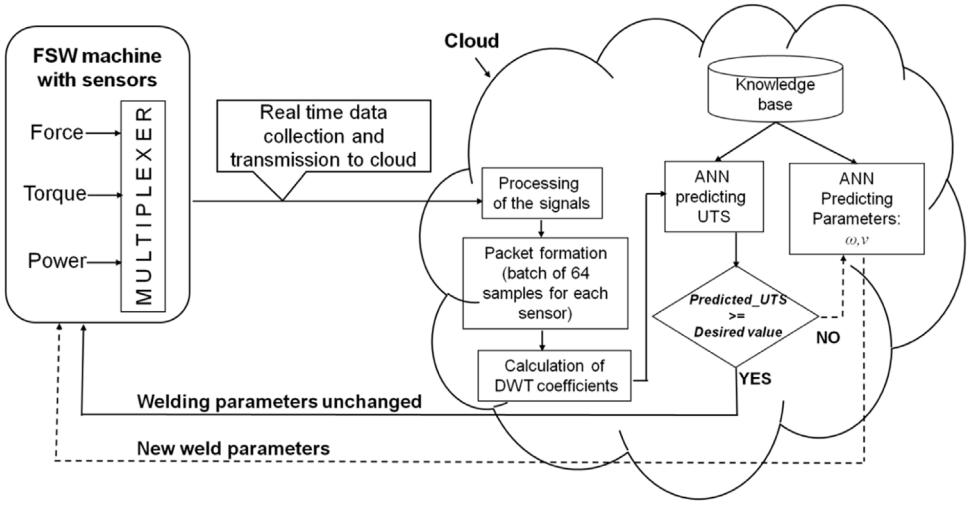

Fig. 3. Diagram of the multi-sensor model.

The reception of weld parameters from cloud to FSW machine is also being performed via TCP/IP. The receiving unit in LABVIEW receives the modified parameters. It then changes ω and v in real time. TCP/IP block for reading and writing are used to receive and send data during the welding process. In order to change the value of ω, 0 is sent first, followed by the desired value. Similarly, for changing v, 1 is sent first, followed by the desired value.

Sensors and data acquisition

As discussed, force and torque are acquired by using a load cell preinstalled in FSW machine, and the power sensor was connected externally, and integrated with the developed interface. The data acquisition rate of force and torque sensors is 10 Hz which is fixed in the machine. In order to have synchronization between the information acquired by using force, torque, and power sensors, the data from power sensor was also acquired at a rate of 10 Hz by using a data acquisition card (NI 6211). A time controlled 4:1 multiplexer is created in the GUI with inputs as: marker value, force, torque, and power data, and the output of this multiplexer is connected as the input to the TCP write block. The marker here is sent as an indication before arrival of every batch of data. The entire welding process has been monitored remotely as the entire server side GUI can be accessed using the remote desktop software X2GO.

Data transmission to cloud

The synchronized data along with a marker is transmitted to cloud in real time at a rate of 8 samples per second. Thus, the streaming data is received in batches, where one batch of data consists of 64 samples of each sensor. These 64 samples were processed through various DSP techniques and meaningful features were extracted from them, which were then sent to an artificial neural network (ANN) for predicting the UTS of the weld in real time. The model is fed with a desired value of the UTS, which is continuously used by the model to compare with the predicted UTS value. In the case, the predicted UTS value is found lesser than the desired value of the UTS; a second ANN predicts the new weld parameters, which forms feedback to the FSW machine to achieve the desired weld quality. If the predicted UTS value is greater than the desired UTS value, the parameters being used for fabrication remains unchanged. In this work, "*Meghamala*", the cloud server of *Indian Institute of Technology Kharagpur* is used. FSW machine is the client utilizing the services being provided by *Meghamala*.

Extraction of meaningful features from signal

Discrete Wavelet Transform (DWT) has been applied on the information acquired from the sensors to extract information about the weld quality. DWT represents a signal in time-frequency domain where the original signal is broken down into various frequency bands, and the effect of each of the frequency band can be analyzed individually. It is advantageous than *Fourier Transform* in a way that the latter technique yields only the frequency information of the signal and does not provide any information about the time of occurrence of those frequencies. DWT is also advantageous than the *Short Time Fourier Transform* technique which although provides a mapping of time and frequencies present in a signal, but utilizes window of fixed width for analyzing the signal. Hence, it fails to accurately analyze the transient signals. Thus, wavelets can provide useful information about transient signals.

The detail coefficients up to three levels, i.e. D1, D2, and D3 of the information acquired from three sensors have been extracted which formed the basis of decision making in cloud. This fact of deriving detail coefficients for predicting weld quality has been taken from the literature [1,14]. Sum of the mean squared error of the coefficients up to the third level has been extracted as the feature to predict the weld quality. The selection of the mother wavelet, levels of decomposition, and feature have been performed as per the literature [1]. The following paragraphs depict graphically the derived features from the three signals, and relate the same with the weld quality.

Fig. 4 shows the image of a sample welded with two sets of process parameters (first set: ω = 600 rpm, and v = 250 mm/min, and second set: ω = 2000 rpm, and v = 50 mm/min), where the first set resembles a defective weld and the second set resembles a defect-free weld with a smooth surface. The idea behind this sort of weld fabrication was to identify defective and defect-free welds with respect to the features from the signals on a same plot. The information acquired from three sensors were processed offline and have been depicted attaching to the weld image shown in Fig. 4. While sudden fluctuations can be observed because of the defects in the first set, almost no fluctuation is seen for the second set.

Fig. 5 represents another defective sample welded with ω = 600 rpm and v = 150 mm/min. Associated with same figure is the plot of the detail coefficients extracted from the three signals. The range of the coefficient's values in case of force sensor can be seen to be approximately higher than 500. At few locations, large fluctuations can also be seen where the value goes above 1000.

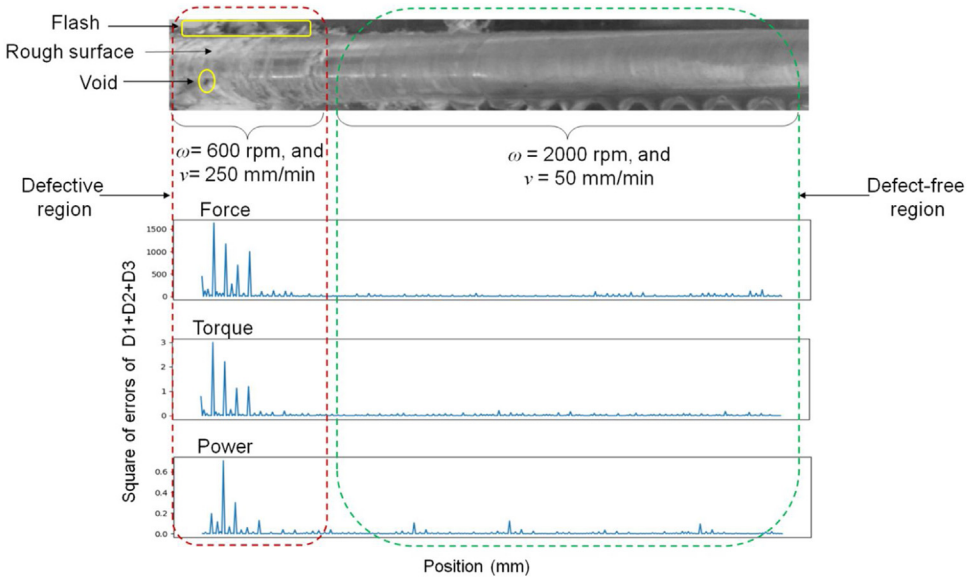

Fig. 4. Plot of detail coefficients extracted from the signals mapped with weld image having defective and defect-free regions.

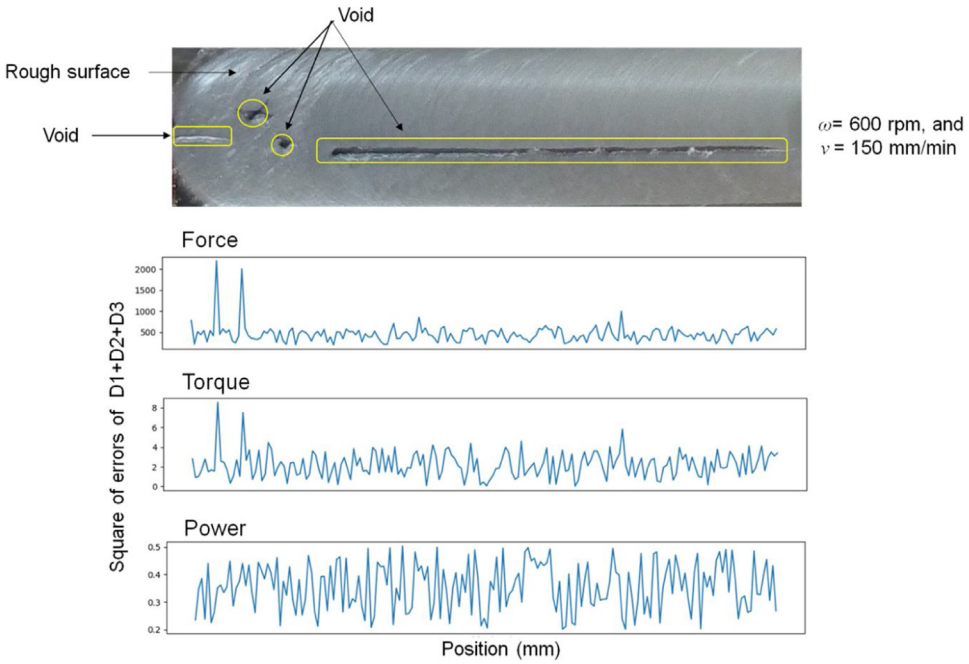

Fig. 5. Plot of detail coefficients extracted from the signals mapped with a defective weld.

Similarly, the value is around 4 for torque and 0.3–0.5 for power, which is much higher than that of the values obtained in Fig. 4 for defect-free region.

Fig. 6 shows the picture of a sample welded with $\omega = 1800$ rpm, and $v = 40$ mm/min resembling a defect-free weld. The corresponding plot of detail coefficients extracted from the three sensors have also been shown in the same figure mapped with the weld image. It can be seen from the figure how the features' values are significantly lower than that of the ones obtained in case of the defective weld (Fig. 5).

The above investigation led to the prediction of weld quality i.e. to know if a weld is with or without defects. For the prediction of UTS, only the D1 coefficients have been considered as they capture most of the information from the signal, and the coefficients at the subsequent levels lose that information due to the down-sampling process. These D1 coefficients have been extracted from data batches containing 64 samples of each sensor which resulted in 35 detail coefficients per batch. Other batch sizes like 32, 64, 128, 256, and 500 were also examined to determine the optimal batch size. The batch size of 32 did not fetch any useful result, 64 and 128 had similar performance, 256 and 500 had good prediction performance but high latency. Therefore, as the present work aims at real-time control, a 64 batch size was found to be the optimal.

ANN modelling

Two ANNs have been modelled, one for predicting the UTS, and other for predicting the modified weld parameters. The ANNs have

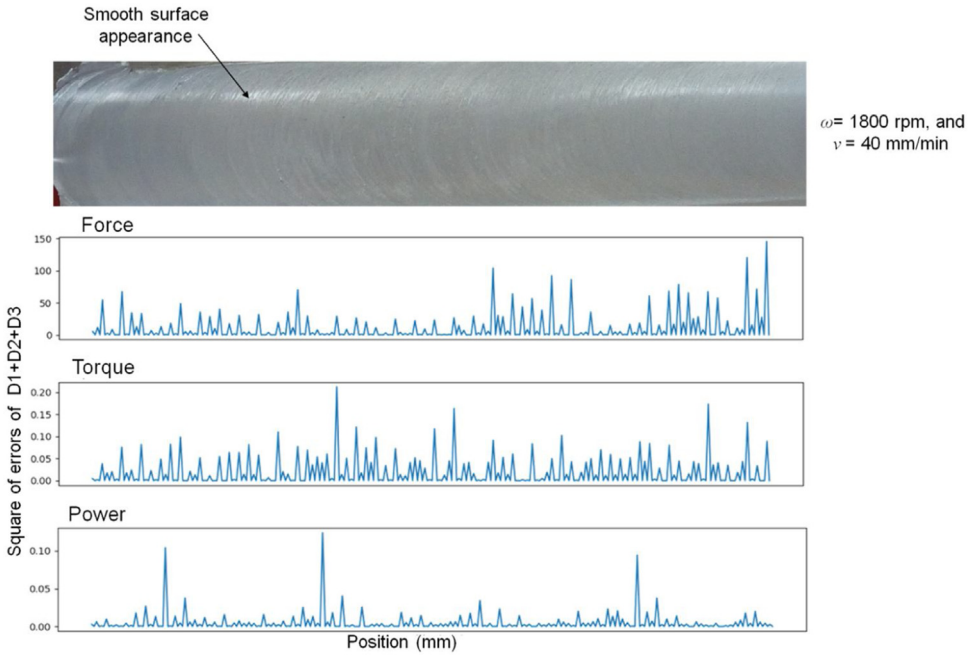

Fig. 6. Plot of detail coefficients extracted from the signals mapped with defect-free weld.

been trained using the *backpropagation* algorithm which operates on a technique named *gradient descent*. This technique searches for the minimum value of error function in the weight space, and the corresponding weights that minimize the error are finally considered as the solution to a given problem. The weights of the edges in the two ANNs were randomly set. The gradient for each training instance within the dataset is determined which results in frequent updates of the network. The momentum coefficient has been selected to be 0.9. The number of hidden layers and the number of hidden neurons in each hidden layer were modelled using *genetic algorithm* (GA) which is a search-based optimization technique. MATLAB toolbox has been used for applying GA. A subset of the welding data consisting of D1 coefficients of force, torque, and power was selected as inputs along with the UTS, and ω and v, as the outputs, for the ANN predicting the UTS and modified parameters, respectively. The chromosomes resemble to the number of neurons in each hidden layer. The initial generation consisted of random numbers of neurons in each hidden layer with some upper bound, and the algorithm predicted the optimum architecture of the ANN. The numbers of hidden layers have been increased from 1, and GA has been applied on each one of the hidden layers. The fitness function selected is mean square error (MSE) between the predicted output and the actual output.

With the above, the optimized architecture of ANN for the UTS prediction has been depicted in Fig. 7. The inputs to this ANN is 105, where 35 numbers of D1 coefficients were of force (f_1 *to* f_{35}), torque (t_1 *to* t_{35}), and power (p_1 *to* p_{35}), respectively. The network comprised of 8 hidden layers, and numbers of hidden neurons in those layers is mentioned in the figure. Fig. 8 depicts the variation of MSE with the increasing number of hidden layers for this ANN which justifies the selection of 8 numbers of hidden layers.

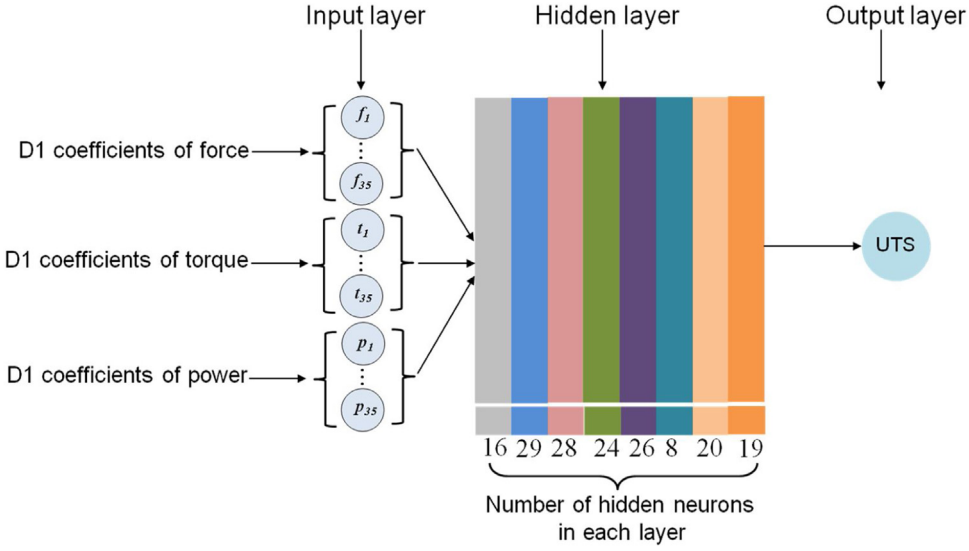

Fig. 7. ANN for prediction of the UTS.

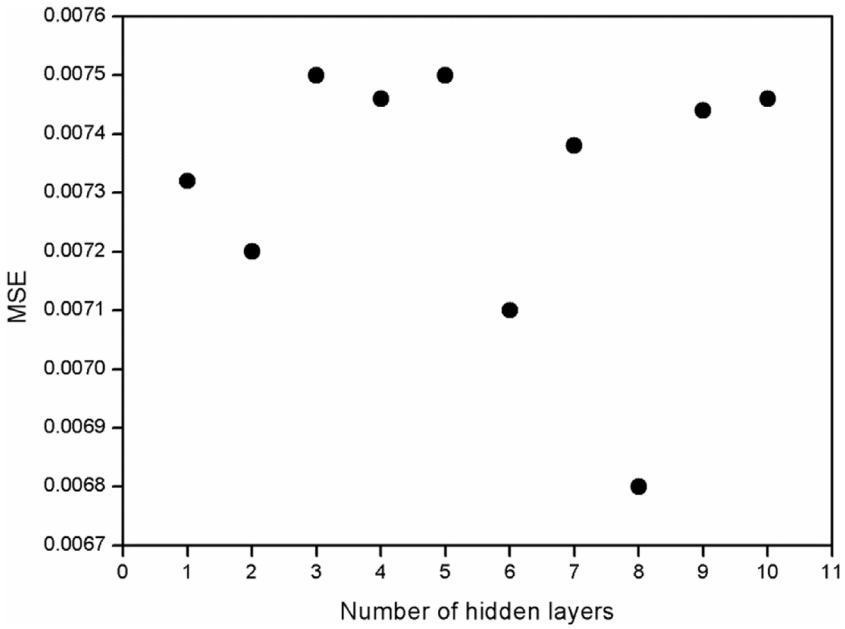

Fig. 8. Variation of MSE with the number of hidden layers for ANN predicting the UTS.

Fig. 9 shows the optimized architecture of ANN for predicting the modified parameters. This network comprised of 10 hidden layers which was selected as per the variation of MSE, shown in Fig. 10.

Results and discussion

This section presents a holistic view of the results obtained by applying the various techniques elaborated in the preceding sections. A number of samples have been welded with different conditions to analyze the efficiency of the developed model.

Welding with improper combination of process parameters

To test the algorithm, a sample was welded (Fig.11) with parameters such that a defective weld will be produced. Those parameters were $\omega = 600$ rpm, and $v = 150$ mm/min. The base materials, tool, machine, and sensors used in these experiments were kept same as described in the section presenting experimental details. The desired value of the UTS fed to the model was 210 MPa. After establishing the connection between the *client* and *server*, the weld fabrication started with the desired UTS value. It can be seen that how the selected weld parameters produced a defective weld with the presence of flash, voids, and rough appearance of the weld surface *(Segment 1)*. The subsequent prediction of the UTS and new weld parameters has been shown in the figure (*Segment 2*, *3* and *4*). A clear improvement in the weld surface appearance can be observed as compared to *Segment 1*. In order to evaluate the efficiency of the prediction, a tensile specimen was cut from the weld sample to determine the deviation from the actual UTS value, and the corresponding prediction error has been mentioned in the figure. The absolute average error of prediction for this case tends to be 4.44%. Hence, it provides clarity as to how this strategy is trying to achieve the

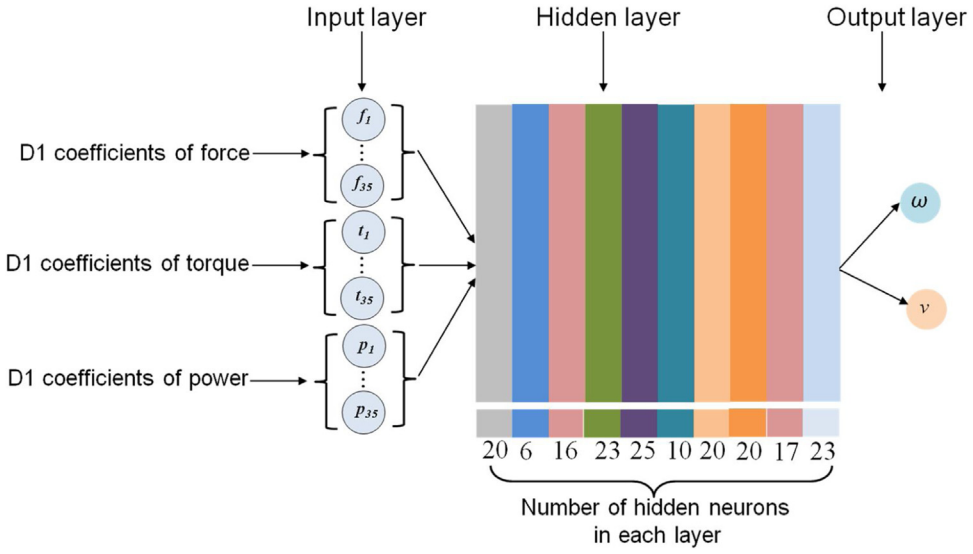

Fig. 9. ANN for prediction of modified parameters.

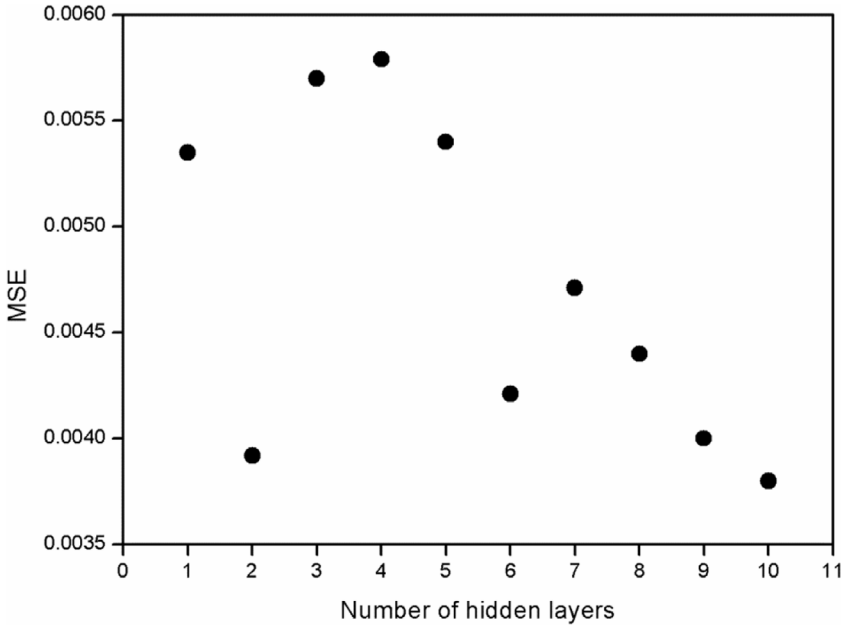

Fig. 10. Variation of MSE with the number of hidden layers for ANN predicting modified parameters.

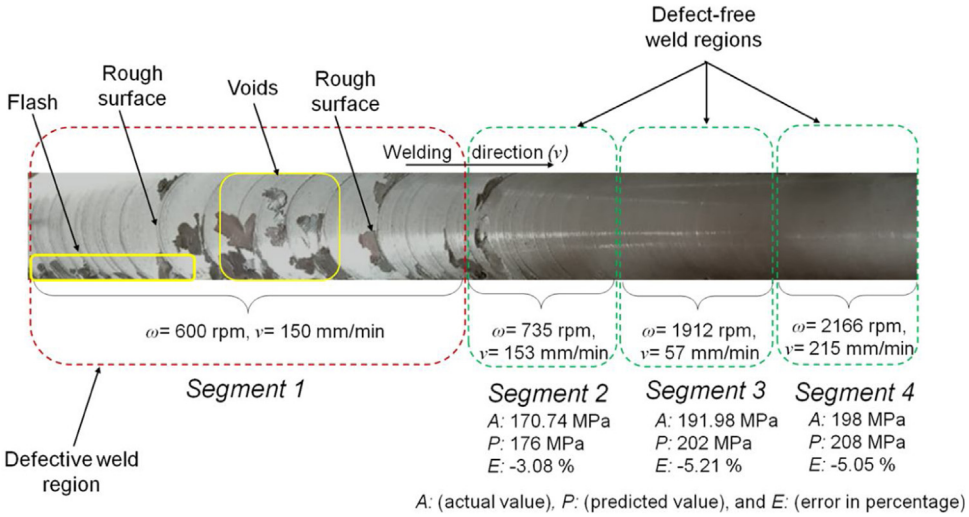

Fig. 11. Real time control of defects during welding with improper parametric combination.

desired UTS value by predicting the weld parameters to the machine based on the features extracted from multiple sensors in real time.

Similarly, another sample was also welded as shown in Fig. 12. The initial parameters for this experiment were so chosen that it was bound to produce a defective weld, and the same is also evident from the weld image which consist of large number of voids and has rough surface appearance *(Segment 1)*. The desired value of UTS fed to the model was 210 MPa. The subsequent predictions of modified weld parameters have been shown in *Segment 2* and *3*, respectively. It can be seen that how the appearance of weld surface improved with subsequent predictions of modified weld parameters. In this case, the absolute average error of prediction is 4.47%.

Welding with optimum conditions

Another sample was welded (Fig. 13) with parameters for which the UTS obtained was 90% of that of the base material. The desired value of UTS was fed as 240 MPa. The fabricated weld had a smooth surface appearance without any surface defects, as expected. The intuition here was that there would not be any prediction as the UTS of the selected parameters is higher than the desired. However, towards the end of the weld, there was a prediction of new process parameters. Thus, just before this prediction, the predicted value of the UTS was less than the desired value (i.e. 208 MPa is the predicted UTS, and 240 MPa is the desired UTS). It is quite evident that the ANN model is always accompanied with some prediction error, which states that even with the predicted value being 239.5 MPa, the model will predict new process parameters. In order to compensate this error, a band for the desired UTS was considered instead of a fixed value.

In order to validate the above mentioned concept, one more sample was welded with the similar set of process parameters as chosen for the weld image shown in Fig. 13 (i.e. $\omega = 1000$ rpm, and $v = 150$ mm/min). However, the desired value of the UTS in this case was a band of value, i.e. 230–240 MPa. The corresponding welded sample has been shown in Fig. 14. With the selected band for the

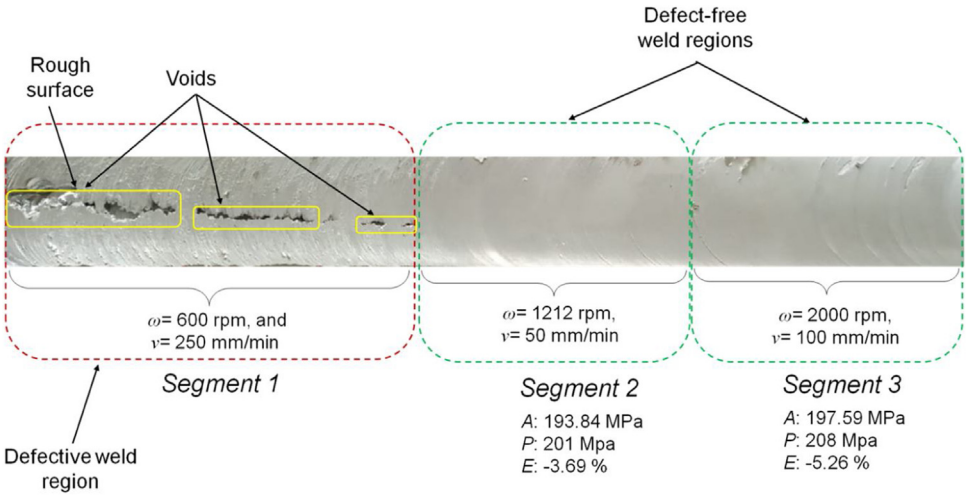

Fig. 12. Real time control of defects during welding with improper parametric combination (another sample).

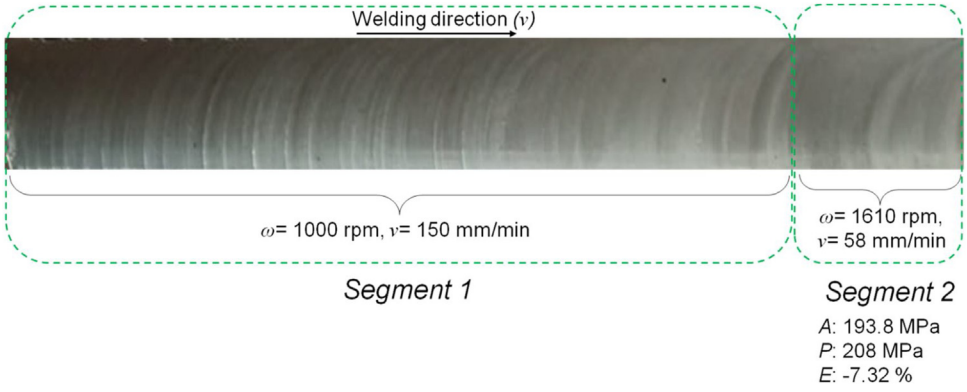

Fig. 13. Picture of the sample welded under optimum conditions with the developed control scheme.

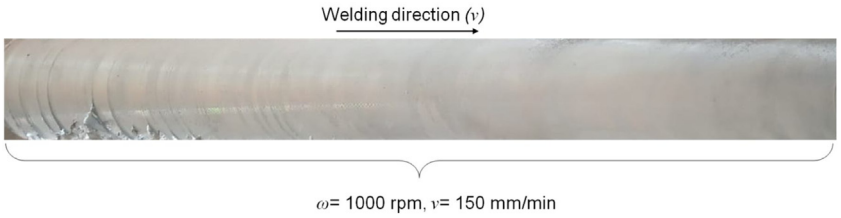

Fig. 14. Picture of the sample welded under optimum conditions and a band of UTS with the developed control scheme.

desired UTS value, the controlled conditions were achieved more profoundly. Thus, it can be stated that, instead of having a fixed value for the desired UTS, a band for the same will make the model avoid errors and ensure its performance.

Effect of usage of multiple sensors over single sensor

In this section, the usage of multiple sensors over a single sensor has been presented. For this, three samples were welded, each one of them being monitored by using the developed algorithm. However, the algorithm here consisted of data being acquired by using only one sensor, i.e. one weld with data acquired from force sensor, one with torque sensor, and the last being with power sensor. For all the three welds, the initial process parameters were kept the same, i.e. ω = 600 rpm, and v = 150 mm/min, as selected for the sample welded with data being acquired from all the three sensors (referring to Fig. 11). For all the three cases, the desired value of UTS was fed as 210 MPa, as selected for the weld employing multiple sensors. Table 2 lists the predicted process parameters, corresponding value of UTS (predicted and actual) for these three welds. It can be observed that for the same length of the workpiece, i.e. for single sensor and multiple sensors case, the numbers of prediction being made in case of single sensor are more than the case of multiple sensors. Since there were quite a number of predictions being made with the individual sensor case, and the combinations of ω and v that were predicted did not differ much from each other, tensile specimen were cut accordingly.

The predicted values of ω and v for single sensor being so close to each other, suggests that the domain of process parameters prediction is limited with the feature values obtained from the signal. However, this was not found in case of multiple sensors. Also, the actual values of the UTS for the sample welded with multiple sensors are more than the sample welded with single sensor. In addition, it can also be observed that while using

Table 2
Predicted process parameters, corresponding predicted and actual value of the UTS during welding with data acquired from a single sensor.

Force					Torque					Power				
ω	v	P	A	E	ω	v	P	A	E	ω	v	P	A	E
2263	56	195	187.5	4.53	1897	128	203	177.6	14.3	2269	58	205	181.2	10.1
2263	84	198			1897	119	203			2279	58	200		
2263	81	195			1897	116	203	178.6	13.6	2281	61	200		
2263	81	215	192.8	11.2	1896	113	203			2282	61	198		
2263	81	214			1897	118	203	177.3	14.4	2279	60	195		
2263	81	212	193.6	8.9	1897	118	203			2285	61	197	194.6	1.4
2246	80	210			–	–	–	–		2282	60	197		
–	–	–	–		–	–	–	–		2275	59	198		
–	–	–	–		–	–	–	–		2280	62	199	195.2	1.94
–	–	–	–		–	–	–	–		2280	61	199		
–	–	–	–		–	–	–	–		2283	59	199		
–	–	–	–		–	–	–	–		2285	59	197		
–	–	–	–		–	–	–	–		2249	60	201		

(ω (rpm), v (mm/min), A-actual UTS and P-predicted UTS (MPa), E- absolute error (%)).

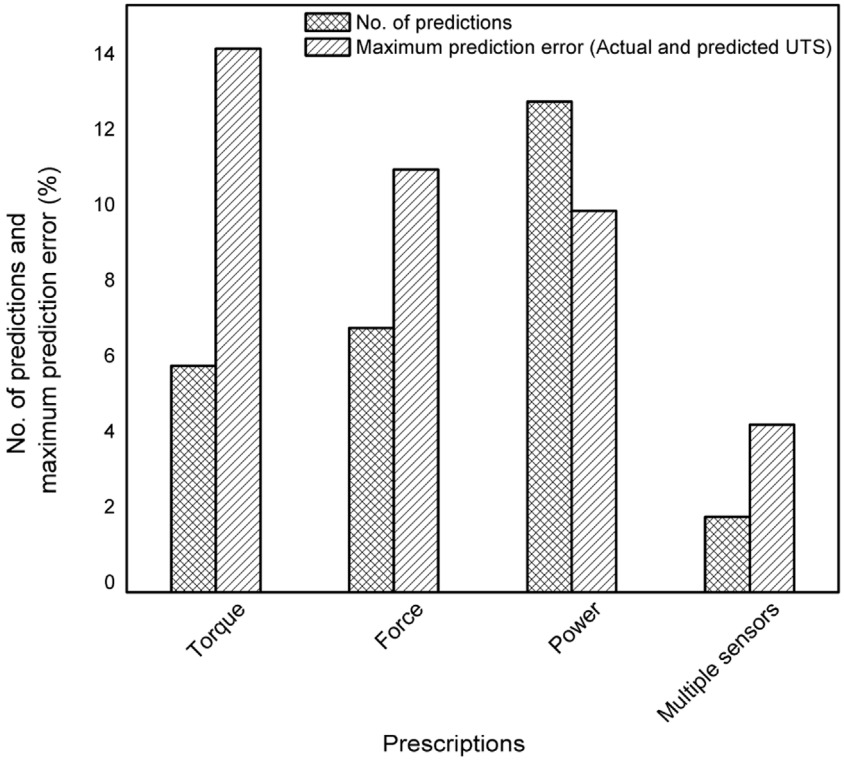

Fig. 15. Effect of multiple sensors over single sensor.

multiple sensors, the prediction error is lesser as compared to single sensor (Fig. 15). Although, the goal of avoiding the occurrence of defects in FSW process is also getting fulfilled by using a single sensor (i.e. force or torque or power), the entire process might be disturbed if that particular sensor starts malfunctioning or produces erroneous data. With multiple sensors installed, one sensor can continuously compensate the malfunctioning of the other.

Welding is a process of value addition which creates structures, components, machines etc. from various raw materials. This algorithm will be useful for several industrial applications as it will help the industry to attain higher levels in quality management. There are certain applications where the strength of the weld is not a huge concern. Instead, there is an emphasis on the aesthetic property of the weld as well. For instance, *"Apple Inc."*, the manufacturer of *"iMac"* utilizes FSW to join its front and back panels [15]. For these computer panels, aesthetic is of higher concern than strength. Thus, the developed model will also be useful for this sort of application. This model can also be applied to other manufacturing process to monitor and control it in real time. However, the objectives such as what are to be controlled in a process and the corresponding signals that can be captured to analyze that effect, required focused research.

Conclusion

A novel technique for remote and real time monitoring and control of FSW process using multiple sensors has been presented in this article. The technique involves computation in cloud which makes the process of control more efficient, reliable, and cost-effective. In future, other sensors such as temperature and vibration can be considered to extract more useful information

about the process, and explore the gathered information to further control the welding process in great detail.

Funding

Department of Heavy Industry, Ministry of Heavy Industries & Public Enterprises, Government of India. Grant number: 12/4/2014 - HE&MT. Industry partner: TATA Consultancy Services.

References

[1] Kumar, U., Yadav, I., Kumari, S., Kumari, K., Ranjan, N., 2015, Defect Identification in Friction Stir Welding Using Discrete Wavelet Analysis. Advances in Engineering Software, 85:43–50. http://dx.doi.org/10.1016/j.advengsoft.2015.02.001.

[2] Kumari, S., Jain, R., Kumar, U., Yadav, I., Ranjan, N., Kumari, K., et al, 2016, Defect Identification in Friction Stir Welding Using Continuous Wavelet Transform. Journal of Intelligent Manufacturing, 1–12. http://dx.doi.org/10.1007/s10845-016-1259-1.

[3] Fleming, P., Lammlein, D., Wilkes, D., Bloodworth, T., Cook, G., Strauss, A., et al, 2008, In-process Gap Detection in Friction Stir Welding. Sensor Review, 1:62–67. http://dx.doi.org/10.1108/02602280810850044.

[4] Chen, C., Kovacevic, R., Jandgric, D., 2003, Wavelet Transform Analysis of Acoustic Emission in Monitoring Friction Stir Welding of 6061 Aluminum. International Journal of Machine Tools, 43:1383–1390. http://dx.doi.org/10.1016/S0890-6955(03)00130-5.

[5] Boldsaikhan, E., Corwin, E.M., Logar, A.M., Arbegast, W.J., 2011, The Use of Neural Network and Discrete Fourier Transform for Real-Time Evaluation of Friction Stir Welding. Applied Soft Computing, 11:4839–4846. http://dx.doi.org/10.1016/j.asoc.2011.06.017.

[6] Subramaniam, S., Narayanan, S., Ashok, S.D., 2013, Acoustic Emission-based Monitoring Approach for Friction Stir Welding of Aluminum Alloy AA6063-T6 with Different Tool Pin Profiles. Proceedings of the Institution of Mechanical Engineers Part B: Journal of Engineering Manufacture, 227:407–416. http://dx.doi.org/10.1177/0954405412472673.

[7] Das, Bipul, Sukhomay Pal, S.B., 2014, Monitoring of Friction Stir Welding Process Through Signals Acquired During the Welding. 5th International and 26th All India Manufacturing Technology, Design and Research Conference (AIMTDR-2014) (December 12th–14th, 2014, IIT Guwahati, Assam, India), pp.1–7.

[8] Cook, G.E., Crawford, R., Clark, D.E., Strauss, A.M., 2004, Robotic Friction Stir Welding. Industrial Robot: An International Journal, 31:55–63. http://dx.doi.org/10.1108/01439910410512000.

[9] Longhurst, W.R., Strauss, A.M., Cook, G.E., Fleming, P.A., 2010, Torque Control of Friction Stir Welding for Manufacturing and Automation. International Journal of Advanced Manufacturing Technology, 51:905–913. http://dx.doi.org/10.1007/s00170-010-2678-3.

[10] Longhurst, W.R., Strauss, A.M., Cook, G.E., 2010, Enabling Automation of Friction Stir Welding: The Modulation of Weld Seam Input Energy by Traverse Speed Force Control. Journal of Dynamic Systems Measurement and Control, 132041002. http://dx.doi.org/10.1115/1.4001795.

[11] Mishra, D., Roy, R.B., Dutta, S., Pal, S.K., Chakravarty, D., 2018, A Review on Sensor Based Monitoring and Control of Friction Stir Welding Process and a Roadmap to Industry 4.0. Journal of Manufacturing Processes, 36:373–397. http://dx.doi.org/10.1016/j.jmapro.2018.10.016.

[12] Mahto, R.P., Kumar, R., Pal, S.K., Panda, S.K., 2018, A Comprehensive Study on Force, Temperature, Mechanical Properties and Micro-Structural Characterizations in Friction Stir Lap Welding of Dissimilar Materials (AA6061-T6 & AISI304). Journal of Manufacturing Processes, 31:624–639. http://dx.doi.org/10.1016/j.jmapro.2017.12.017.

[13] Chauhan, P., Jain, R., Pal, S.K., Singh, S.B., 2018, Modeling of Defects in Friction Stir Welding Using Coupled Eulerian and Lagrangian Method. Journal of Manufacturing Processes, 34:158–166. http://dx.doi.org/10.1016/j.jmapro.2018.05.022.

[14] Roy, R.B., Ghosh, A., Bhattacharyya, S., Mahto, R.P., Kumari, K., Pal, S.K., et al, 2018, Weld Defect Identification in Friction Stir Welding Through Optimized Wavelet Transformation of Signals and Validation Through X-ray Micro-CT Scan. International Journal of Advanced Manufacturing Technology, 99:623–633. http://dx.doi.org/10.1007/s00170-018-2519-3.

[15] Sangalli, G., Lemos, G.V.B., Martinazzi, D., Lessa, C.Rde L., Beskow, A.B., Reguly, A., 2019, Towards Qualification of Friction Stir Welding to AA5083-O and AA5052-O Aluminum Alloys. Materials Research, 22:1–8. http://dx.doi.org/10.1590/1980-5373-mr-2019-0349.